

- 1 Balancing adipocyte production and lipid metabolism to treat
- 2 diabetes-associated obesity with a novel proteoglycan from
- 3 Ganoderma lucidum
- 5 YingXin Wang ¹, Fanzhen Yu ¹, Xinru Zheng ¹, Jiaqi Li ¹, Zeng Zhang ²,
- 6 Qianqian Zhang 1, Jieying Chen 1, Yanming He 2,*, Hongjie Yang 2,* and Ping
- 7 Zhou ^{1,*}.

- 8 State Key Laboratory of Molecular Engineering of Polymers, Department of
- 9 Macromolecular Science, Fudan University, Shanghai 200433, China
- ² Yueyang Hospital of Integrated Traditional Chinese and Western Medicine,
- 11 Shanghai University of Traditional Chinese Medicine, Shanghai 200437, China
- * Correspondence to: pingzhou@fudan.edu.cn (P.Z.), Tel/Fax: +86-21-31244038;
- 13 yanghongjie1964@aliyun.com (H.Y.); heyanming176@163.com (Y.H.)

Abstract 15 Obesity is often accompanied by metabolic disorder and insulin resistance, resulting in 16 type 2 diabetes. Based on previous findings, FYGL, a natural hyperbranched 17 proteoglycan extracted from the G. lucidum fruiting body, can decrease blood glucose 18 and reduce body weight in diabetic mice. In this article, the underlying mechanism of 19 20 FYGL in ameliorating diabetes-associated obesity was further investigated both in vivo 21 and in vitro. FYGL upregulated expression of metabolic genes related to fatty acid biosynthesis, fatty acid β-oxidation and thermogenesis; downregulated the expression 22 of insulin resistance-related genes; and significantly increased the number of beige 23 24 adipocytes in db/db mice. In addition, FYGL inhibited preadipocyte differentiation of 25 3T3-L1 cells by increasing the expression of FABP-4. FYGL not only promoted fatty acid synthesis but also more significantly promoted triglyceride degradation and 26 metabolism by activating the AMPK signalling pathway, therefore preventing fat 27 accumulation, balancing adipocyte production and lipid metabolism, and regulating 28 metabolic disorders and unhealthy obesity. FYGL could be used as a promising 29 pharmacological agent for the treatment of metabolic disorder-related obesity. 30 31 **Keywords**: metabolic disorder; obesity; diabetes; *Ganoderma lucidum*; adipocytes; 32 lipid metabolism; 3T3-L1; AMPKα signalling pathway 33 34

15 Introduction

36

Type 2 diabetes mellitus (T2DM) is a chronic degenerative disease, and 60% of T2DM 37 patients are obese as a result of metabolic disorder and insulin resistance as well as 38 impaired energy homoeostasis [1-6]. Adipose tissues play an important role in surplus 39 energy storage and energy metabolism [7]. Adipose tissue comprises white adipose 40 41 tissue (WAT) and brown or beige adipose tissue (BAT). WAT mainly functions to store 42 fat in the form of lipid droplets and secrete adipokines to regulate the metabolism of tissues such as muscle and liver tissues [8]. BAT mainly functions to dissipate excess 43 energy through thermogenesis to maintain a stable body weight, and it secretes many 44 batokines to affect the physiology of a variety of organ systems and tissues, such as the 45 liver, heart and muscle [9,10]. Accumulating evidence has suggested that a high ratio 46 of white to beige adipocytes is associated with insulin resistance [3,5]. 47 Adipocytes are differentiated from preadipocytes; therefore, many studies have 48 focused on inhibiting the differentiation of preadipocytes in addition to lipid 49 metabolism to treat obesity [11,12]. Mesenchymal stem cells (MSCs) undergo a two-50 51 step process to differentiate into adipocytes: MSCs first differentiate into preadipocytes, and preadipocytes continue to differentiate into mature adipocytes [13,14]. During 52 adipogenesis, peroxisome proliferator-activated receptor gamma (PPARy) and 53 CCAAT/enhancer-binding protein α (C/EBP α) are marker proteins for preadipocytes 54 differentiating into mature adipocytes [15,16]. Subsequently, fatty acids are synthesized 55 in conjunction with the expression of acetyl-CoA carboxylase (ACCα) and fatty acid 56 synthase (FAS). Moreover, mature adipocytes further synthesize triglycerides, which 57

aggregate to form lipid droplets [17]. In addition, the triglycerides in lipid droplets are degraded in conjunction with the expression of adipose triglyceride lipase (ATGL), hormone-sensitive lipase (HSL), and lipoprotein lipase (LPL) [18,19], which are regulated by the AMP-activated protein kinase α (AMPK α) signalling pathway; thermogenesis in BAT is also regulated by this pathway [20,21]. Based on these results, finding an effective agent to regulate metabolic disorders and alleviate diabetesassociated obesity is very important. Some antiobesity drugs, such as orlistat and liraglutide, have been applied clinically in recent years [22,23]. Orlistat controls body weight by inhibiting pancreatic lipases but has side effects, such as faecal incontinence and flatulence. [24]. Liraglutide controls body weight by suppressing gastric emptying and food intake, increasing satiety, and limiting nutrient absorption by increasing pancreatic \(\beta \) cell proliferation, regenerating β cells, and alleviating insulin resistance but also has side effects such as nausea, vomiting, and diarrhoea [25]. Metformin, a first-line therapeutic agent for diabetes, is an AMPK activator capable of increasing insulin sensitivity and decreasing body weight, but it also has side effects such as abdominal distension, diarrhoea and gastrointestinal intolerance [26]. In recent years, some natural medicinal plants have been used in the treatment of obesity and metabolic diseases because of their safety [27]. Hibiscus rosa-sinensis flowers were reported to be capable of decreasing obesity by reducing adipogenesis and activating AMPK to promote fatty acid oxidation [12]. Momordica charantia extracts can activate the AMPK signalling pathway, reduce adipogenic gene expression and peroxisome proliferator-activated receptor (PPAR)

58

59

60

61

62

63

64

65

66

67

68

69

70

71

72

73

74

75

76

77

78

signalling in adipose tissue, and increase lipid oxidation in adipose tissue, thereby 80 reducing obesity and insulin resistance [28,29]. In addition, cannabidiol can promote 81 adipocyte browning for the treatment of metabolic diseases [30]. 82 Previously, Teng et al. extracted a proteoglycan called *FYGL* (Fudan-Yueyang G. 83 lucidum) from the fruiting body of Ganoderma lucidum, a traditional Chinese medicinal 84 85 herb used for immunoregulation, anti-inflammation, anti-diabetes and anti-86 cancer[31,32]. The dominant sequence of FYGL is shown in Figure 1 [33,34]. FYGL is a hyperbranched proteoglycan with a molecular weight of 2.6×10⁵ Da and a saccharide: 87 protein ratio of 77:17 [33,34]. FYGL has been proven capable of decreasing fasting 88 89 blood glucose through inhibition of the activity of protein tyrosine phosphatase 1 B 90 (PTP1B), an insulin resistance receptor, both in vitro [35] and in vivo [36,37], as well as reducing body weight in ob/ob mice [38]. However, the underlying mechanism by 91 which FYGL controls body weight is unknown. 92 In this work, the mechanism of FYGL antidiabetic associated with obesity was 93 investigated both in vivo and in vitro. In in vivo studies, adipose tissue from db/db 94 diabetic mice was used to analyse the expression of genes related to fatty acid 95 biosynthesis and metabolism, thermogenesis, and insulin sensitivity, which are 96 beneficial for BAT functions. In in vitro studies, the 3T3-L1 cell line was used to 97 investigate the underlying mechanism by which FYGL alleviates obesity. 3T3-L1 cells 98 are preadipocytes and normally differentiate into mature adipocytes [39]. The effects 99 100 of FYGL on preadipocyte differentiation and mature adipocyte lipid metabolism were investigated by multiple approaches, including analysis of protein expression in 101

preadipocytes and the signalling pathways of lipid metabolism in mature adipocytes.

Materials and Methods

Materials

103

104

Fruiting bodies of G. lucidum grown in northeastern China were purchased from 105 Leiyunshang Pharmaceutical Co. Ltd (Shanghai, China). The preparation of FYGL was 106 described in previous work [36]. Dulbecco's modified Eagle's medium (DMEM), foetal 107 108 bovine serum (FBS), and penicillin/streptomycin antibiotics were purchased from Gibco Co. Ltd (USA). 3T3-L1 cells were obtained from Procell Life Science & 109 Technology Co. Ltd (Wuhan, China). Fluorescein isothiocyanate (FITC), 4',6-110 diamidino-2-phenylindole (DAPI), rhodamine-labelled phalloidin and super ECL 111 112 detection reagent were provided by Yeasen Co. Ltd (Shanghai, China). A cell counting kit-8 (CCK-8), a modified oil red O staining kit, a bicinchoninic acid (BCA) kit, 113 newborn calf serum (NCS), RIPA lysis buffer, dexamethasone, 3-Isobutyl-1-114 methylxanthine (IBMX), paraformaldehyde, Triton X-100, anti-rabbit IgG (H + L), and 115 a horseradish peroxidase (HRP)-labelled secondary antibody were purchased from 116 Beyotime Co. Ltd (Shanghai, China). Dimethyl sulfoxide (DMSO) was provided by 117 Sigma-Aldrich (Taufkirchen, Germany). Triglyceride (TG) assay kits were obtained 118 from Jiancheng Bioengineering Institute (Nanjing, China). The RNAprep pure cell kit 119 was acquired from TIANGEN Biotech Co. Ltd (Beijing, China). The HiScript III All-120 in-one RT SuperMix kit (#R333) and Taq Pro Universal SYBR qPCR Master Mix kit 121 (#Q712) were purchased from Vazyme Biotech Co. Ltd (Nanjing, China). Primary 122 antibodies against peroxisome proliferator-activated receptor gamma (PPAR, A11183), 123

```
lipoprotein lipase (LPL, A16252), and \beta\text{-actin} (AC026) were purchased from ABclonal
124
      Technology Co. Ltd (Wuhan, China). Primary antibodies against CCAAT/enhancer-
125
      binding protein α (C/EBPα, ab40764), fatty acid synthase (FAS, ab128870), fatty acid
126
      binding protein 4 (FABP-4, ab92501), adipose triglyceride lipase (ATGL, ab109251),
127
      AMPKα1 (ab32047), AMPKα1 (phospho T183) + AMPKα2 (phospho T172) (p-
128
129
      AMPKα, ab133448) were purchased from Abcam (Cambridge, MA, USA). Primary
130
      antibodies against hormone-sensitive lipase (HSL, #4107) were purchased from Cell
131
      Signaling Technology (CST, Beverly, MA, USA).
132
      Animal trial
      All male BKS-DB (db/db) mice (4 weeks old) and wild-type BKS-DB (db/m) mice
133
134
      were purchased from GemPharmatech Co. Ltd, Nanjing, China. Mice were housed in
      the specific pathogen-free (SPF) Animal Experimental Center of the School of
135
      Pharmacy, Fudan University, at a constant temperature (22 \pm 2 °C) on a 12 h/12 h
136
      light/dark cycle and were provided standard food and water. All animal trials were
137
      conducted following protocols approved by the Fudan University Institutional Animal
138
139
      Care and Use Committee. Subsequent experimental procedures were performed
      according to the method described in previous works [40,41]. Mice were randomly
140
      divided into six groups (n = 12 mice per group): (1) normal group (wild-type BKS mice
141
      treated with saline); (2) control group (db/db) mice treated with saline); (3) positive
142
      control group (db/db mice treated with 225 mg/kg metformin); (4) low-dose group
143
144
      (db/db mice treated with 225 mg/kg FYGL); (5) middle-dose group (db/db mice treated
      with 450 mg/kg FYGL); and (6) high-dose group (db/db mice treated with 900 mg/kg
145
```

FYGL). After 7 weeks of drug treatment, all the mice were sacrificed.

Histopathological analysis of beige adipose tissue

148 Beige adipose tissue (BAT) was extracted from the scapulae of db/db mice and were

fixed, sectioned, and mounted. The sections were stained with haematoxylin and eosin

(H&E) and observed by microscopy (NanoZoomer 2.0-HT, Japan). Adipocyte numbers

are shown as ratios of the adipocyte number to the area of the selected region (a

randomly selected circle with an area of 0.1 mm²) in the images.

RNA sequencing (RNA-seq) analysis of BAT

Total RNA was extracted from beige adipose tissue. RNA purity was checked using a NanoPhotometer® spectrophotometer (IMPLEN, CA, USA). RNA integrity was assessed using the RNA Nano 6000 Assay Kit for the Bioanalyzer 2100 system (Agilent Technologies, CA, USA). Sequencing libraries were generated using the NEBNext® UltraTM RNA Library Prep Kit for Illumina® (NEB, USA) following the manufacturer's recommendations, and index codes were added to attribute sequences to each sample. Clustering of the index-coded samples was performed on a cBot Cluster Generation System using TruSeq PE Cluster Kit v3-cBot-HS (Illumina) according to the manufacturer's instructions. After cluster generation, the library preparations were sequenced on the Illumina NovaSeq platform, and 150 bp paired-end reads were generated. Every group was analysed with three biological replicates. Differential expression analyses between two conditions or groups (two biological replicates per condition) were performed using the DESeq2 R package (1.16.1). Genes with an adjusted P value of < 0.05 determined by DESeq2 were considered differentially

expressed. Gene Ontology (GO) enrichment analysis of the differentially expressed genes was implemented in the cluster Profiler R package, in which gene length bias was corrected. GO terms with a corrected P value of less than 0.05 were considered significantly enriched with differentially expressed genes. The clusterProfiler R package was used to test the statistical enrichment of the differentially expressed genes in KEGG pathways. Cell culture and treatment 3T3-L1 preadipocytes were maintained in DMEM supplemented with 10% NCS and 1% penicillin-streptomycin (basal medium I, BMI). When the cells were confluent (Day 0), adipocyte differentiation was induced by treatment with a cocktail of 5 μg/mL insulin, 1 µM dexamethasone, and 0.5 mM isobutyl methylxanthine in DMEM supplemented with 10% FBS and 1% penicillin-streptomycin (differentiation medium I, DMI). After 48 h (Day 2), the medium was changed to DMEM containing 10% FBS, 1% penicillin-streptomycin, and 5 μg/mL insulin for 48 h (differentiation medium II, DMII). On Day 4, insulin was removed from the medium, and the cells were maintained in DMEM supplemented with 10% FBS and 1% penicillin-streptomycin (basal medium II, BMII), and the medium was changed every two days thereafter [42]. During differentiation, cells were treated with different concentrations of FYGL (0, 50, 100, 200, 400, and 800 µg/mL). Undifferentiated cells cultured in BMI were used as the blank control group, and differentiated cells cultured in BMI without FYGL were used as the model groups.

Uptake of FYGL in 3T3-L1 cells

168

169

170

171

172

173

174

175

176

177

178

179

180

181

182

183

184

185

186

187

188

190	Three milligrams of FITC fluorescence agent was dissolved in 0.3 mL of DMSO to
191	prepare a FITC solution with a concentration of 10 mg/mL, and then the solution was
192	diluted to 1 mg/mL with sodium buffer (SB). FYGL (10 mg) was dissolved in 10 mL
193	SB to form a 1 mg/mL FYGL solution, which was mixed with the diluted FITC solution
194	at a volume ratio of 10:1. The mixture was stirred at low temperature (ice bath) to allow
195	the formation of fluorescent FITC-FYGL complexes. After the coupling reaction was
196	allowed to proceed overnight, the solution was dialyzed with a 1 kDa dialysis bag to
197	filter free FITC and then cryodesiccated.
198	3T3-L1 cells were seeded on microscope cover glasses in a 24-well plate at a
199	density of 1×10^4 cells per well and were incubated with FITC-FYGL complexes (200
200	μg/mL) for 4 h. Nuclei and F-actin (filamentous actin) in 3T3-L1 cells were stained by
201	DAPI and phalloidin-TRITC (phalloidin-tetramethyl rhodamine), respectively. Cell
202	images were acquired with a C2 ⁺ laser scanning confocal microscope (Nikon, Japan).
203	Moreover, 3T3-L1 cells were treated with the indicated concentrations of FITC-FYGL
204	$(0, 50, 100, 200, 400, 800 \mu g/mL)$ for 4 h, and then the fluorescence intensity was
205	determined by flow cytometry (Gallios, Beckman Coulter) to visualize the uptake of
206	FYGL in the cells.
207	Measurement of cell viability
208	Cell viability was measured by a cell counting kit-8 (CCK-8) assay. In brief, 3T3-L1
209	cells were plated into 96-well plates at a density of 5×10^3 cells per well and incubated
210	to near confluence. Some cells were incubated in DMI with different concentrations of
211	6 FYGL (0, 100, 200, 400, and 800 μg/mL) for 24 h. After treatment for 24 h, the medium

was discarded, and fresh DMI containing CCK-8 solution was added to the 96-well 212 213 plates. Approximately 1 h later, a multimode microplate reader (Cytation3, BioTek, 214 U.S.A.) was used to measure the optical density (OD) at 450 nm. Triglyceride quantification 215 Triglyceride (TG) concentrations were determined using a commercial kit (Jiancheng 216 217 Bioengineering Institute, China). Briefly, differentiated 3T3-L1 cells were washed 218 twice with phosphate-buffered saline (PBS) and harvested by scraping from the culture plate in PBS containing 1% Triton X-100 on Day 6. Cell homogenates were obtained 219 220 by sonication, and TG concentrations were determined using a commercial kit 221 according to the manufacturer's instructions. Protein concentrations were measured 222 using the bicinchoninic acid (BCA) protein assay kit (Beyotime, China) and used for quantification of proteins in samples. 223 Oil red O staining and quantification 224 Lipid accumulation in cells was measured by oil red O staining. Differentiated 3T3-L1 225 cells were subjected to oil red O staining with modified oil red O staining kits 226 (Beyotime, China). Briefly, the cells were washed with phosphate-buffered saline (PBS, 227 pH 7.4) and then fixed with 10% (v/v) paraformaldehyde at room temperature for 10 228 min. Then, the fixation solution was removed, and the cells were washed twice with 229 PBS. The cells were immersed in washing solution for 20 secs. After the washing 230 solution was discarded, modified oil red O was added and incubated with the cells at 231 232 room temperature for 20 min. Then, the staining solution was removed, and the cells were washed with washing solution once and PBS twice. Finally, cells stained with oil 233

234	red O were examined via a polarizing microscope (DM2500P, Leica, Germany). In
235	addition to this gross evaluation, the dye was dissolved in 60% isopropanol solution,
236	and the absorbance was measured at 510 nm.
237	RNA extraction and RT-qPCR analysis
238	Total RNA was isolated from differentiated 3T3-L1 cells using RNAprep pure cell kits
239	(TIANGEN, China) according to the manufacturer's instructions. Conversion of total
240	RNA to single-stranded cDNA was performed using HiScript III All-in-one RT
241	SuperMix Kits (Vazyme, China). The series of primers shown in Table 1 for
242	amplification of β -actin (as an internal reference), C/EBP α , FABP4, ATGL, and LPL
243	were synthesized by Sangon Co. The primers were mixed with the cDNA templates,
244	and qPCR was then performed with a Taq Pro Universal SYBR qPCR Master Mix kit
245	(Vazyme, China) on a qPCR instrument (Bio-Rad, Germany) to amplify the DNA of
246	$C/EBP\alpha$, FABP4, ATGL, and LPL. The melt curves of the cDNA were analysed to
247	determine the specificity of amplification, and quantification of relative mRNA levels
248	was performed using the $2^{-\Delta\Delta Ct}$ method with normalization to β -actin mRNA.
249	Protein extraction and immunoblot analysis
250	Immunoblot analysis was performed according to the method described in a previous
251	report with a minor modification [43]. Differentiated 3T3-L1 cells were lysed in RIPA
252	lysis buffer and centrifuged (12000 \times g, 10 min, 4 °C). Proteins in the lysates were
253	separated by 10% SDS-PAGE and transferred to polyvinylidene fluoride membranes.
254	Then, the membranes were blocked in TBST/5% nonfat dry milk powder; incubated
255	overnight at 4 °C with antibodies against FABP4, PPAR γ , CEBP α , AMPK α , p-AMPK α ,

256	ATGL, HSL, LPL, and β-actin; and incubated with a goat anti-rabbit secondary
257	antibody at room temperature for 1 h. Finally, enhanced chemiluminescence solution
258	(ECL) was used to detect the proteins on the membranes. The luminescence signals
259	were recorded with a Chemiscope 3300 mini (Clinx Science Instruments, China). Data
260	were collected from three independent experiments.
261	18 Statistical analysis
262	All data were analysed by SPSS 20.0 (SPSS, Inc., U.S. and are expressed as the mean
263	± S.D. values. One-way ANOVA followed by the Bonferroni correction was performed
264	to analyse the statistical significance of differences among the groups. A value of $P <$
265	0.05 was considered statistically significant.
266	Results and Discussion
267	1 Effect of <i>FYGL</i> on BAT histopathology <i>in vivo</i>
268	Teng previously proved that FYGL can decrease triglycerides and total cholesterol in
269	SD rats with STZ-induced diabetes [33], which is closely related to lipid biosynthesis
270	and metabolism. In the present work, BAT in db/db mice was subjected to
271	histopathological analysis. Figure 2A shows that the size of beige adipocytes was larger
272	31
	and the numbers were lower in the control group than in the normal group, whereas
273	and the numbers were lower in the control group than in the normal group, whereas treatment with metformin and FYGL reduced the size of adipocytes. Semiquantitative
273 274	
	treatment with metformin and FYGL reduced the size of adipocytes. Semiquantitative
274	treatment with metformin and FYGL reduced the size of adipocytes. Semiquantitative analysis of H&E staining in Figure 2B showed that FYGL significantly increased the

with body mass index [44]; the smaller the size and the greater the number of beige adipocytes, the healthier the body [45-47]. Ouellet et al. demonstrated that the activity of beige adipocytes is positively correlated with the level of glucose uptake in cells. which modulates the blood glucose content [48]. Therefore, increasing the number or activation of beige adipocytes could be a potential approach to treat type 2 diabetesassociated obesity [49]. Consistent with those studies, the results of this study showed that beige adipocytes were significantly enlarged and increased in number in db/db mice, while these changes were significantly reversed after *FYGL* treatment. Effect of FYGL on lipid metabolism in vivo Type 2 diabetes is strongly associated with genes of lipid metabolism[50]. In this work, BAT transcriptome sequencing was performed to explore the potential molecular mechanism of lipid metabolism in vivo. As shown in Figure 3A, the screening results of the differentially expressed genes (DEGs) showed that the ratio of upregulated: downregulated: all significant differentially expressed genes was approximately 0.5:0.5:1 in the metformin and FYGL groups compared with the control group, nearly the same as the ratio in the normal group compared to the control group. Figure 3B shows the hierarchical clustering heatmap. The large coloured square patterns represent the upregulated or downregulated genes in the different groups. The change in colour from blue to red indicates a change in the gene expression from downregulation to upregulation. The narrow columns on the left show the pathway-related genes. Figure 3B shows that the colour patterns of the DEGs in the control group were different from those in the normal group for most genes except Ppp1r3b, while the colour patterns in

278

279

280

281

282

283

284

285

286

287

288

289

290

291

292

293

294

295

296

297

298

300 the FYGL group were similar to those in the normal group. From the pathway indication 301 in the upper-left corner in Figure 3B, it can be seen that the DEGs were involved in the pathways of fatty acid synthesis (black), fatty acid oxidation (green), insulin resistance 302 303 (yellow), and thermogenesis (purple). As shown in Figure 3B, FYGL increased the mRNA levels of Ppp1r3b, Fasn, 304 Acaca, CPT2, and Acadl in the BAT of db/db mice compared to those in the control 305 306 group. The *Ppp1r3b* gene encodes protein phosphatase 1, which is a critical protein in 307 glycogen metabolism regulated by insulin [51]. The Fasn (encoding FAS [52]) and 308 Acaca (encoding ACCα [53]) genes are involved in fatty acid synthesis [52,53]. CPT2 (encoding CPT-II, carnitine palmitoyl transferase II [54]) and Acadl (encoding ACADL, 309 acyl-CoA dehydrogenase long chain [55]) are involved in the β-oxidation of long-chain 310 311 fatty acids in mitochondria [54,55]. The imbalance between fatty acid synthesis and 312 degradation can lead to dyslipidaemia, diabetes and cardiovascular disease [56, 57]. Transcript analysis of those genes in BAT indicated that FYGL could upregulate fatty 313 acid metabolism in vivo. Additionally, as shown in Figure 3B, FYGL upregulated fatty 314 315 acid degradation genes (CPT2 and Acadl) more significantly than fatty acid synthesis genes (Fasn and Acaca). In addition, as shown in Figure 3C, FYGL increased the levels 316 of Cd81 (encoding CD81 [58]) and Slc25a4 (encoding SLC25A4 [59]) compared to 317 those in the control group, and the levels of these mRNAs in the FYGL group were even 318 higher than those in the metformin group. CD81 is a marker of beige adipocyte 319 320 progenitors. The absence of CD81 leads to diet-induced obesity, insulin resistance, and adipose tissue inflammation [58]. SLC25A4, a mitochondrial ATP/ADP transporter, 321

regulates BAT thermogenesis through UCP1-independent mechanisms [60]. Beige adipocytes can produce heat by metabolizing fatty acids. Transcriptome analysis indicated that FYGL could increase the expression of thermogenesis genes (Cd81 and Slc25a4) in BAT, as indicated by the transition from blue to red in Figure 3C. Furthermore, FYGL and metformin increased the mRNA levels of Akt2 (encoding AKT2 [61]) and Slc2a4 (encoding GLUT-4, glucose transporter-4 [62]), as shown in Figure 3B. Deficiency of AKT2 and GLUT-4 leads to type 2 diabetes and insulin resistance [61,63]. The GO (Gene Ontology) database is a comprehensive database describing gene functions and includes the biological process (BP), cellular component (CC), and molecular function (MF) ontological categories. Figure 4A shows the bubble plot of the biological processes in the GO enrichment analysis (FYGL vs. control), where the redder the dot is, the more significant the enrichment of the biological process. Figure 4A shows that DEGs were mainly enriched in terms related to the biological processes of cellular respiration, fatty acid metabolism, tricarboxylic acid metabolism, fatty acid oxidation, etc., and that FYGL restored BAT functions in db/db mice through those biological processes. Figure 4B is a directed acyclic graph (DAG, FYGL vs. control) of the GO biological process enrichment analysis results and indicates the relationship of functions from upregulated to downregulated biological processes. Figure 4C shows that the biological processes were eventually refined to include only fatty acid metabolism and cellular respiration. FYGL upregulated the fatty acid metabolism

process and promoted thermogenesis in brown adipocytes.

322

323

324

325

326

327

328

329

330

331

332

333

334

335

336

337

338

339

340

341

342

KEGG enrichment analysis aims to identify connections between differentially
expressed genes and signalling pathways. Figure 4C shows the bubble plot of the
signalling pathways in the KEGG enrichment analysis (FYGL vs. control), where the
redder the dot is, the more significant the enrichment of the signalling pathway. Figure
4B shows that DEGs were predominantly enriched in signalling pathways related to
oxidative phosphorylation, thermogenesis, the citrate cycle (TCA cycle), fatty acid
metabolism, and fatty acid biosynthesis. The data in Figure 4B suggest that FYGL
promotes the functions of BAT through those signalling pathways.
These findings indicated that FYGL could balance fatty acid biosynthesis and
metabolism to effectively dissipate energy, therefore reducing insulin resistance and
increasing insulin sensitivity <i>in vivo</i> .
Cellular uptake of FYGL
Cellular uptake of FYGL To reveal the underlying mechanisms of FYGL in mediating biological functions,
To reveal the underlying mechanisms of <i>FYGL</i> in mediating biological functions, investigations at the cellular level are necessary. Figure 5A shows the uptake of <i>FYGL</i>
To reveal the underlying mechanisms of FYGL in mediating biological functions,
To reveal the underlying mechanisms of <i>FYGL</i> in mediating biological functions, investigations at the cellular level are necessary. Figure 5A shows the uptake of <i>FYGL</i>
To reveal the underlying mechanisms of $FYGL$ in mediating biological functions, investigations at the cellular level are necessary. Figure 5A shows the uptake of $FYGL$ (200 µg/mL and 400 µg/mL) in 3T3-L1 cells, as measured by confocal laser scanning microscopy, where green fluorescence was found in the cells cultured with FITC- $FYGL$, indicating that $FYGL$ could be taken up well into 3T3-L1 cells. Moreover, the results
To reveal the underlying mechanisms of $FYGL$ in mediating biological functions, investigations at the cellular level are necessary. Figure 5A shows the uptake of $FYGL$ (200 µg/mL and 400 µg/mL) in 3T3-L1 cells, as measured by confocal laser scanning microscopy, where green fluorescence was found in the cells cultured with FITC- $FYGL$,
To reveal the underlying mechanisms of <i>FYGL</i> in mediating biological functions, investigations at the cellular level are necessary. Figure 5A shows the uptake of <i>FYGL</i> (200 μg/mL and 400 μg/mL) in 3T3-L1 cells, as measured by confocal laser scanning microscopy, where green fluorescence was found in the cells cultured with FITC- <i>FYGL</i> , indicating that <i>FYGL</i> could be taken up well into 3T3-L1 cells. Moreover, the results of flow cytometric analysis of <i>FYGL</i> uptake in 3T3-L1 cells are shown in Figure 5B and Figure 5C; the peak of the curve shifted to the right as the FITC- <i>FYGL</i>
To reveal the underlying mechanisms of $FYGL$ in mediating biological functions, investigations at the cellular level are necessary. Figure 5A shows the uptake of $FYGL$ (200 µg/mL and 400 µg/mL) in 3T3-L1 cells, as measured by confocal laser scanning microscopy, where green fluorescence was found in the cells cultured with FITC- $FYGL$, indicating that $FYGL$ could be taken up well into 3T3-L1 cells. Moreover, the results of flow cytometric analysis of $FYGL$ uptake in 3T3-L1 cells are shown in Figure 5B
To reveal the underlying mechanisms of <i>FYGL</i> in mediating biological functions, investigations at the cellular level are necessary. Figure 5A shows the uptake of <i>FYGL</i> (200 μg/mL and 400 μg/mL) in 3T3-L1 cells, as measured by confocal laser scanning microscopy, where green fluorescence was found in the cells cultured with FITC- <i>FYGL</i> , indicating that <i>FYGL</i> could be taken up well into 3T3-L1 cells. Moreover, the results of flow cytometric analysis of <i>FYGL</i> uptake in 3T3-L1 cells are shown in Figure 5B and Figure 5C; the peak of the curve shifted to the right as the FITC- <i>FYGL</i>

To examine the cytotoxicity of FYGL in 3T3-L1 adipocytes, cell viability was measured 366 367 using the CCK-8 assay. Adipocytes were treated with various concentrations of FYGL 368 (0-800 μg/mL). The CCK-8 assay results shown in Figure 5D demonstrate that FYGL 369 had no obvious cytotoxicity at concentrations up to 800 µg/mL. Effect of FYGL on the accumulation of intracellular triglycerides and lipids 370 371 Lipid accumulation in adipocytes is a hallmark of adipogenesis. Mature differentiated 372 cells accumulate triglycerides, which then converge to form lipid droplets (LDs). FYGL significantly decreased the triglyceride content, as shown in Figure 6A. Moreover, cell 373 374 differentiation and lipid accumulation can be identified by oil red O staining and triglyceride assays. Figure 6B shows that the number of lipid droplets (red staining) 375 376 was markedly increased in cells cultured in differentiation medium (DM) but was significantly decreased when the cells were cultured with FYGL (200-400 µg/mL), and 377 Figure 6C quantitatively shows the effect of FYGL on lipid droplet accumulation. 378 Excessive accumulation of lipid droplets in adipocytes leads to obesity and insulin 379 resistance [17]. FYGL inhibited triglyceride accumulation and lipid droplets in 380 381 differentiated adipocytes. The mechanism of inhibition was further investigated as follows. 382 Effect of FYGL on the expression of adipogenic and lipolytic genes and proteins 383 Several reports have shown that peroxisome proliferator-activated receptor y (PPARy) 384 and CCAAT/enhancer-binding protein α (C/EBPα) are marker proteins of adipocyte 385 differentiation and adipogenesis [64-66]. Tali et al. found that fatty acid binding 386 protein-4 (FABP-4)-null preadipocytes can enhance PPARγ expression and activity, 387

388	while the overexpression of FABP-4 inhibits PPAR γ expression and adipogenesis [67].
389	Furuhashi et al. further found that FABP-4-null mice exhibit decreased lipolysis in
390	adipocytes and pancreatic $\boldsymbol{\beta}$ cells and reduced insulin secretion [68]. To reveal the
391	mechanisms by which $FYGL$ inhibits the accumulation of intracellular triglycerides and
392	lipids, the effect of $FYGL$ on the expression of adipogenic and lipolytic genes and
393	proteins was investigated. Interestingly, FYGL significantly increased the transcript
394	level of FABP-4 (Figure 7A) in 3T3-L1 preadipocytes and considerably increased the
395	transcript level of $C/EBP\alpha$ in adipocytes cultured in differentiation medium (Figure 7B).
396	Moreover, FYGL increased the mRNA level of lipolytic genes, such as ATGL (Figure
397	7C) and LPL (Figure 7D).
398	Furthermore, Western blotting was used to analyse the protein expression of FABP-
399	4, PPARγ, and C/EBPα, as shown in Figure 8A. FYGL greatly increased FABP-4
400	expression, as shown in Figure 8B, and markedly decreased PPARγ and C/EBPα
401	expression, as shown in Figure 8C and 8D. This work proved that FYGL could inhibit
402	the differentiation of 3T3-L1 preadipocytes and promote lipolysis in adipocytes,
403	therefore reducing lipid droplet accumulation.
404	Effect of FYGL on lipid metabolism and the AMPKα signalling pathway
405	Studies have shown that fatty acid synthase (FAS) plays an important role in lipogenic
406	pathways, which are involved in fatty acid biosynthesis [69]. In addition, the $\mbox{AMPK}\alpha$
407	signalling pathway also plays a critical role in lipolysis [20,70,71]. Activating the
408	AMPK signalling pathway can increase the activity of the lipases ATGL, HSL, and
409	LPL, thus promoting the utilization of lipid storage [20,70-72]. ATGL and HSL catalyse

triglyceride degradation, releasing the fatty acids in lipid droplets of adipocytes [73], while adipocytes secrete LPL to degrade triglycerides in VLDL in vessels [74]. As shown in Figure 9A and 9B, *FYGL* increased the protein expression of FAS. Additionally, *FYGL* increased the phosphorylation of AMPKα (Figure 9C&D) and consequently increased the protein expression of lipolysis markers, such as ATGL (Figure 9E), HSL (Figure 9F), and LPL (Figure 9G).

The results of this study indicated that *FYGL* promoted the degradation of lipid droplets in mature adipocytes by activating the AMPKα signalling pathway. In addition, *FYGL* increased the protein levels of ATGL (Figure 9E) and HSL (Figure 9F) by 2-fold compared with that of FAS (Figure 9B) and by 1.5-fold compared with those in the control group at concentrations higher than 200 μg/mL. Therefore, *FYGL* upregulated lipolysis more significantly than fatty acid biosynthesis, consistent with the animal experiment results. Taken together, the results of the study on the cellular level showed that *FYGL* could inhibit lipid accumulation by both suppressing the differentiation of preadipocytes and promoting the degradation of lipid droplets in mature adipocytes to alleviate metabolically unhealthy obesity.

Conclusion

In conclusion, this study showed that FYGL could increase the number of beige adipocytes and restore adipocyte morphology, thereby alleviating metabolic disorders in db/db mice. The mechanism by which FYGL alleviates metabolic disorders involves the balance between fatty acid biosynthesis and metabolism to effectively dissipate energy in beige adipocytes. In addition, FYGL inhibited the differentiation of

432	preadipocytes by increasing FABP-4 gene expression and decreasing PPAR γ and
433	C/EBPα gene levels. Moreover, FYGL promoted adipocyte browning by upregulating
434	Cd81 gene expression. Furthermore, $FYGL$ increased the levels of the lipolysis-related
435	proteins ATGL, HSL and LPL by activating the AMPK $\!\alpha$ signalling pathway, therefore
436	accelerating lipid metabolism in mature adipocytes. Importantly, these findings proved
437	that FYGL, a proteoglycan, could improve metabolic disorders in vivo by targeting both
438	preadipocytes and mature adipocytes. The mechanistic profile of FYGL in the treatment
439	of diabetes-associated obesity is shown in Figure 10. FYGL could be used as a
440	promising agent to treat lipid metabolism disorders and obesity in the clinic.
441 442	
443	Declarations
444	Ethics approval and consent to participate: The study was conducted in accordance
444 445	Ethics approval and consent to participate: The study was conducted in accordance with the Declaration of Helsinki and approved by the Ethics Committee of Fudan
445	with the Declaration of Helsinki and approved by the Ethics Committee of Fudan
445 446	with the Declaration of Helsinki and approved by the Ethics Committee of Fudan
445 446 447	with the Declaration of Helsinki and approved by the Ethics Committee of Fudan University (No. FE21038, 5 March 2021). Consent for publication: Not applicable.
445 446 447 448	with the Declaration of Helsinki and approved by the Ethics Committee of Fudan University (No. FE21038, 5 March 2021).
445 446 447 448 449	with the Declaration of Helsinki and approved by the Ethics Committee of Fudan University (No. FE21038, 5 March 2021). Consent for publication: Not applicable.
445 446 447 448 449 450	with the Declaration of Helsinki and approved by the Ethics Committee of Fudan University (No. FE21038, 5 March 2021). Consent for publication: Not applicable. Availability of data and materials: The data presented in this study are available
445 446 447 448 449 450 451	with the Declaration of Helsinki and approved by the Ethics Committee of Fudan University (No. FE21038, 5 March 2021). Consent for publication: Not applicable. Availability of data and materials: The data presented in this study are available

455	Funding: This research was funded by the National Natural Science Foundation of
456	China (Nos. 21374022 and 81374032); National Health Commission of the People's
457	Republic of China (No. 2017ZX09301006); Science and Technology Commission of
458	Shanghai Municipality (No. 17401902700); Clinical Research Plan of SHDC (No.
459	SHDC12019124); and Shanghai Collaborative Innovation Center of Industrial
460	Transformation of Hospital TCM Preparation.
461	_
462	Authors' contributions: Y.W: design, acquisition, analysis and interpretation of data,
463	writing of the draft and final manuscript version. F.Y: interpretation of data, revision of
464	the draft. X.Z: revision of the draft. J.L: analysis of data. Z.Z: interpretation of data.
465	Q.Z: revision of the draft. J.C: analysis of data. Y.H: interpretation of data, funding
466	support. H.Y: design of the work, funding support. P.Z: design of the work, funding
467	support, writing, reviewing and editing of the manuscript. All authors read and
468	approved the final manuscript.
469	
470	Acknowledgements: Not applicable.
471	

- 472 References
- 473 1. Chatterjee S, Khunti K, Davies MJ: **Type 2 diabetes.** *The Lancet* 2017, **389:**2239-2251.
- Tong Y, Xu S, Huang L, Chen C: **Obesity and insulin resistance: Pathophysiology and treatment.** *Drug Discovery Today* 2022, **27:**822-830.
- Nathan DM: Diabetes Advances in Diagnosis and Treatment. Jama-Journal of the American
 Medical Association 2015, 314:1052-1062.
- Dhurandhar NV: What is obesity? International Journal of Obesity 2022, 46:1081-1082.
- Czech MP: Mechanisms of insulin resistance related to white, beige, and brown adipocytes.
 Molecular Metabolism 2020, 34:27-42.
- Gustafson B, Hedjazifar S, Gogg S, Hammarstedt A, Smith U: Insulin resistance and impaired
 adipogenesis. Trends in Endocrinology & Metabolism 2015, 26:193-200.
- 483 7. Dhurandhar NV: What is obesity? International Journal of Obesity 2022.
- Romao JM, Guan LL: Chapter 21 Adipogenesis and Obesity. In MicroRNA in Regenerative
 Medicine. Edited by Sen CK. Oxford: Academic Press; 2015: 539-565
- Hansen Jacob B, Kristiansen K: Regulatory circuits controlling white versus brown
 adipocyte differentiation. Biochemical Journal 2006, 398:153-168.
- 488 10. Yang FT, Stanford KI: **Batokines: Mediators of Inter-Tissue Communication (a Mini-Review).** Current Obesity Reports 2022, 11:1-9.
- 490 11. Wu M, Liu D, Zeng R, Xian T, Lu Y, Zeng G, Sun Z, Huang B, Huang Q: **Epigallocatechin-3-**
- 491 gallate inhibits adipogenesis through down-regulation of PPARγ and FAS expression
 492 mediated by PI3K-AKT signaling in 3T3-L1 cells. European Journal of Pharmacology 2017,
- 493 **795:**134-142.
- Lingesh A, Paul D, Naidu VGM, Satheeshkumar N: AMPK activating and anti adipogenic
 potential of Hibiscus rosa sinensis flower in 3T3-L1 cells. Journal of Ethnopharmacology
- 496 2019, **233:**123-130.
- 497 13. Otto TC, Lane MD: Adipose development: from stem cell to adipocyte. Crit Rev Biochem
 498 Mol Biol 2005, 40:229-242.
- Tang QQ, Lane MD: Adipogenesis: from stem cell to adipocyte. Annu Rev Biochem 2012,
 81:715-736.
- 501 15. Cristancho AG, Lazar MA: Forming functional fat: a growing understanding of adipocyte
 502 differentiation. Nature Reviews Molecular Cell Biology 2011, 12:722-734.
- 503 16. Lehrke M, Lazar MA: The Many Faces of PPARγ. Cell 2005, 123:993-999.
- Sun Z, Gong J, Wu L, Li P: Chapter 14 Imaging Lipid Droplet Fusion and Growth. In
 Methods in Cell Biology. Volume 116. Edited by Yang H, Li P: Academic Press; 2013: 253-268
- Bosch M, Parton RG, Pol A: Lipid droplets, bioenergetic fluxes, and metabolic flexibility.
 Seminars in Cell & Developmental Biology 2020, 108:33-46.
- 508 19. Klemm RW, Ikonen E: **The cell biology of lipid droplets: More than just a phase.** Seminars in Cell & Developmental Biology 2020, **108:**1-3.
- 510 20. Herzig S, Shaw RJ: **AMPK: guardian of metabolism and mitochondrial homeostasis.**511 Nature Reviews Molecular Cell Biology 2018, **19:**121-135.
- 512 21. López M: EJE PRIZE 2017: Hypothalamic AMPK: a golden target against obesity?
 513 European Journal of Endocrinology 2017, 176:R235-R246.
- Aaseth J, Ellefsen S, Alehagen U, Sundfør TM, Alexander J: Diets and drugs for weight loss
 and health in obesity An update. Biomedicine & Pharmacotherapy 2021, 140:111789.

- 516 23. Lingvay I, Sumithran P, Cohen RV, Le Roux CW: **Obesity management as a primary** 517 **treatment goal for type 2 diabetes: time to reframe the conversation.** *The Lancet* 2021.
- Liu TT, Liu XT, Chen QX, Shi Y: Lipase Inhibitors for Obesity: A Review. Biomedicine and
 Pharmacotherapy 2020, 128.
- Drucker DJ: Mechanisms of Action and Therapeutic Application of Glucagon-like Peptide 1. Cell Metab 2018, 27:740-756.
- 522 26. Foretz M, Guigas B, Viollet B: **Understanding the glucoregulatory mechanisms of**523 **metformin in type 2 diabetes mellitus.** *Nature Reviews Endocrinology* 2019, **15**:569-589.
- Ali Esmail A-S, Muayad Hussein A, Kareema Helal S: Medicinal plants for the treatment of
 obesity and overweight: A review. World Journal of Biology Pharmacy and Health Sciences
 2022, 10:001-010.
- Huang HL, Hong YW, Wong YH, Chen YN, Chyuan JH, Huang CJ, Chao PM: Bitter melon
 (Momordica charantia L.) inhibits adipocyte hypertrophy and down regulates lipogenic
 gene expression in adipose tissue of diet-induced obese rats. Br J Nutr 2008, 99:230-239.
- 530 29. Ramachandra Shobha C, Prashant V, Akila P, Chandini R, Nataraj Suma M, Basavanagowdappa
 531 H: Fifty Percent Ethanolic Extract of Momordica charantia Inhibits Adipogenesis and
 532 Promotes Adipolysis in 3T3-L1 Pre-Adipocyte Cells. Rep Biochem Mol Biol 2017, 6:22-32.
- 533 30. Parray HA, Yun JW: **Cannabidiol promotes browning in 3T3-L1 adipocytes.** *Molecular and Cellular Biochemistry* 2016, **416:**131-139.
- Subhasree PDBaRS: The Sacred Mushroom "Reishi"-A Review. American-Eurasian Journal
 of Botany 2008, 1 (3): 107-110, 200.
- Bishop KS, Kao CHJ, Xu Y, Glucina MP, Paterson RRM, Ferguson LR: From 2000years of
 Ganoderma lucidum to recent developments in nutraceuticals. Phytochemistry 2015,
 114:56-65.
- Teng BS, Wang CD, Zhang D, Wu JS, Pan D, Pan LF, Yang HJ, Zhou P: Hypoglycemic effect
 and mechanism of a proteoglycan from ganoderma lucidum on streptozotocin-induced
 type 2 diabetic rats. Eur Rev Med Pharmacol Sci 2012, 16:166-175.
- Pan D, Wang L, Chen C, Hu B, Zhou P: Isolation and characterization of a hyperbranched
 proteoglycan from Ganoderma Lucidum for anti-diabetes. Carbohydrate Polymers 2015,
 117:106-114.
- Yu F, Wang Y, Teng Y, Yang S, He Y, Zhang Z, Yang H, Ding C-F, Zhou P: Interaction and
 Inhibition of a Ganoderma lucidum Proteoglycan on PTP1B Activity for Anti-diabetes.
 ACS Omega 2021, 6:29804-29813.
- Teng B-S, Wang C-D, Yang H-J, Wu J-S, Zhang D, Zheng M, Fan Z-H, Pan D, Zhou P: A
 Protein Tyrosine Phosphatase 1B Activity Inhibitor from the Fruiting Bodies of
 Ganoderma lucidum (Fr.) Karst and Its Hypoglycemic Potency on Streptozotocin-Induced
 Type 2 Diabetic Mice. Journal of Agricultural and Food Chemistry 2011, 59:6492-6500.
- Yang Z, Wu F, He Y, Zhang Q, Zhang Y, Zhou G, Yang H, Zhou P: A novel PTP1B inhibitor
 extracted fromGanoderma lucidumameliorates insulin resistance by regulating IRS1 GLUT4 cascades in the insulin signaling pathway. Food & Function 2018, 9:397-406.
- Yang Z, Zhang Z, Zhao J, He Y, Yang H, Zhou P: Modulation of energy metabolism and
 mitochondrial biogenesis by a novel proteoglycan fromGanoderma lucidum. RSC
 Advances 2019, 9:2591-2598.
- 559 39. Vohra MS, Ahmad B, Serpell CJ, Parhar IS, Wong EH: Murine in vitro cellular models to

- better understand adipogenesis and its potential applications. Differentiation 2020, 115:62 84.
- Zhang Y, Pan Y, Li J, Zhang Z, He Y, Yang H, Zhou P: Inhibition on α-Glucosidase Activity
 and Non-Enzymatic Glycation by an Anti-Oxidative Proteoglycan from Ganoderma
 lucidum. Molecules 2022, 27:1457.
- Pan Y, Yuan S, Teng Y, Zhang Z, He Y, Zhang Y, Liang H, Wu X, Li J, Yang H, Zhou P:
 Antioxidation of a proteoglycan from Ganoderma lucidum protects pancreatic β-cells
 against oxidative stress-induced apoptosis in vitro and in vivo. International Journal of
 Biological Macromolecules 2022, 200:470-486.
- Zebisch K, Voigt V, Wabitsch M, Brandsch M: Protocol for effective differentiation of 3T3 L1 cells to adipocytes. Analytical Biochemistry 2012, 425:88-90.
- Liang H, Pan Y, Teng Y, Yuan S, Wu X, Yang H, Zhou P: A proteoglycan extract from
 Ganoderma Lucidum protects pancreatic beta-cells against STZ-induced apoptosis.
 Bioscience, Biotechnology, and Biochemistry 2020, 84:2491-2498.
- 574 44. Cypess AM, Lehman S, Williams G, Tal I, Rodman D, Goldfine AB, Kuo FC, Palmer EL, Tseng
 575 Y-H, Doria A, .:t al: Identification and Importance of Brown Adipose Tissue in Adult
 576 Humans. New England Journal of Medicine 2009, 360:1509-1517.
- Stock MJ, Cinti S: ADIPOSE TISSUE | Structure and Function of Brown Adipose Tissue.
 In Encyclopedia of Food Sciences and Nutrition (Second Edition). Edited by Caballero B.
 Oxford: Academic Press; 2003: 29-34
- Virtanen KA: Adipose Tissue: Structure and Function of Brown Adipose Tissue. In
 Encyclopedia of Food and Health. Edited by Caballero B, Finglas PM, Toldrá F. Oxford:
 Academic Press; 2016: 30-34
- Lidell ME, Betz MJ, Leinhard OD, Heglind M, Elander L, Slawik M, Mussack T, Nilsson D,
 Romu T, Nuutila P, .:t al: Evidence for two types of brown adipose tissue in humans. Nature
 Medicine 2013, 19:631-634.
- Ouellet V, Routhier-Labadie A, Bellemare W, Lakhal-Chaieb L, Turcotte E, Carpentier AC,
 Richard D: Outdoor Temperature, Age, Sex, Body Mass Index, and Diabetic Status
 Determine the Prevalence, Mass, and Glucose-Uptake Activity of 18F-FDG-Detected BAT
 in Humans. The Journal of Clinical Endocrinology & Metabolism 2011, 96:192-199.
- 590 49. Kajimura S, Bruce, Seale P: Brown and Beige Fat: Physiological Roles beyond Heat
 591 Generation. Cell Metabolism 2015, 22:546-559.
- 59. Kane JP, Pullinger CR, Goldfine ID, Malloy MJ: Dyslipidemia and diabetes mellitus: Role of
 lipoprotein species and interrelated pathways of lipid metabolism in diabetes mellitus.
 Current Opinion in Pharmacology 2021, 61:21-27.
- 595 51. Ceperuelo-Mallafré V, Ejarque M, Serena C, Duran X, Montori-Grau M, Rodríguez MA, Yanes
 596 O, Núñez-Roa C, Roche K, Puthanveetil P, .:t al: Adipose tissue glycogen accumulation is
 597 associated with obesity-linked inflammation in humans. Molecular Metabolism 2016, 5:5 598 18.
- Wallace M, Metallo CM: Tracing insights into de novo lipogenesis in liver and adipose
 tissues. Seminars in Cell & Developmental Biology 2020, 108:65-71.
- Munday MR: Regulation of mammalian acetyl-CoA carboxylase. Biochem Soc Trans 2002,
 30:1059-1064.
- 603 54. Hsiao Y-S, Jogl G, Esser V, Tong L: Crystal structure of rat carnitine palmitoyltransferase

- 604 II (CPT-II). Biochemical and Biophysical Research Communications 2006, 346:974-980.
- 605 55. Chen Y, Ren Q, Zhou Z, Deng L, Hu L, Zhang L, Li Z: **HWL-088**, a new potent free fatty 606 acid receptor 1 (FFAR1) agonist, improves glucolipid metabolism and acts additively with 607 metformin in ob/ob diabetic mice. *Br J Pharmacol* 2020, **177**:2286-2302.
- Jaiswal M, Schinske A, Pop-Busui R: Lipids and lipid management in diabetes. Best Practice
 & Research Clinical Endocrinology & Metabolism 2014, 28:325-338.
- Taskinen M-R, Borén J: New insights into the pathophysiology of dyslipidemia in type 2
 diabetes. Atherosclerosis 2015, 239:483-495.
- Oguri Y, Shinoda K, Kim H, Alba DL, Bolus WR, Wang Q, Brown Z, Pradhan RN, Tajima K,
 Yoneshiro T, .:t al: CD81 Controls Beige Fat Progenitor Cell Growth and Energy Balance
 via FAK Signaling. Cell 2020, 182:563-577.e520.
- Clémençon B, Babot M, Trézéguet V: The mitochondrial ADP/ATP carrier (SLC25 family):
 Pathological implications of its dysfunction. Molecular Aspects of Medicine 2013, 34:485-493.
- 60. Cohen P, Kajimura S: The cellular and functional complexity of thermogenic fat. Nature
 Reviews Molecular Cell Biology 2021, 22:393-409.
- 620 61. Hay N: **Akt isoforms and glucose homeostasis the leptin connection.** *Trends in Endocrinology & Metabolism* 2011, **22:**66-73.
- 622 62. Corrêa-Giannella ML, Machado UF: **SLC2A4gene: a promising target for**623 **pharmacogenomics of insulin resistance.** *Pharmacogenomics* 2013, **14:**847-850.
- 624 63. Li G, Zhang L: miR-335-5p aggravates type 2 diabetes by inhibiting SLC2A4 expression.

 625 Biochemical and Biophysical Research Communications 2021, 558:71-78.
- Rosen ED, Macdougald OA: Adipocyte differentiation from the inside out. Nature Reviews
 Molecular Cell Biology 2006, 7:885-896.
- Ali AT, Hochfeld WE, Myburgh R, Pepper MS: Adipocyte and adipogenesis. Eur J Cell Biol
 2013, 92:229-236.
- 630 66. Otto TC, Lane MD: **Adipose Development: From Stem Cell to Adipocyte.** Critical Reviews in Biochemistry and Molecular Biology 2005, **40:**229 242.
- 632 67. Garin-Shkolnik T, Rudich A, Hotamisligil GS, Rubinstein M: FABP4 Attenuates PPARγ and
 633 Adipogenesis and Is Inversely Correlated With PPARγ in Adipose Tissues. Diabetes 2014,
 634 63:900-911.
- 69. Berndt J, Kovacs P, Ruschke K, Klöting N, Fasshauer M, Schön MR, Körner A, Stumvoll M,
 638 Blüher M: Fatty acid synthase gene expression in human adipose tissue: association with
 639 obesity and type 2 diabetes. Diabetologia 2007, 50:1472-1480.
- Grabner GF, Xie H, Schweiger M, Zechner R: Lipolysis: cellular mechanisms for lipid
 mobilization from fat stores. Nature Metabolism 2021, 3:1445-1465.
- Wang Y, Rodrigues B: Intrinsic and extrinsic regulation of cardiac lipoprotein lipase
 following diabetes. Biochimica et Biophysica Acta (BBA) Molecular and Cell Biology of
 Lipids 2015, 1851:163-171.
- Walther TC, Farese RV: Lipid Droplets and Cellular Lipid Metabolism. Annual Review of
 Biochemistry 2012, 81:687-714.
- 647 73. Ahmadian M, Abbott Marcia J, Tang T, Hudak Carolyn SS, Kim Y, Bruss M, Hellerstein Marc K,

648		Lee H-Y, Samuel Varman T, Shulman Gerald I, .:t al: Desnutrin/ATGL Is Regulated by
649		AMPK and Is Required for a Brown Adipose Phenotype. Cell Metabolism 2011, 13:739-
650		748.
651	74.	Borén J, Taskinen M-R, Björnson E, Packard CJ: Metabolism of triglyceride-rich lipoproteins
652		in health and dyslipidaemia. Nature Reviews Cardiology 2022, 19:577-592.
653		
654		
655		
656		
657		

658	
659	

(A)

(B)

Figure 1 (A) The dominant polysaccharide sequence of FYGL characterized by chemical analysis and NMR spectroscopy[34]. Rs represents the carbohydrate residues of $\rightarrow 2,4$)- α -L-Rhap- $(1\rightarrow$, $\rightarrow 6$ - β -D-Galp- $1\rightarrow$, Araf- $(1\rightarrow$ or $\rightarrow 3,6)$ - β -D-Galp- $(1\rightarrow$. Protein moieties are covalently bonded with carbohydrate moieties by Ser and Thr residues in the -O- linkage. (B) The dominant sequence of the protein moieties of FYGL characterized by mass spectrometry.

(A)

(B)

Figure 2 Histopathological analysis of adipocytes in brown adipose tissues. (A) Representative images of H&E-stained brown adipose tissues, magnification $100\times$. The scale bar represents 250 µm. (B) Semiquantitative analysis of the adipocyte number per area in BAT by Image-Pro Plus 6.0 software. The mean \pm S.D. values are presented (n = 6; ***P < 0.001 vs. normal; $^{\#}P$ < 0.05, $^{\#}P$ < 0.01, $^{\#\#}P$ < 0.001 vs. control).

664 (A) (B) Figure 3 Transcriptome analysis of RNA sequencing of BAT in the normal, metformin, and FYGL groups compared to the control group. (A) DEG counts. (B) Hierarchical clustering heatmap of the expression profile of the DEGs. 665



Figure 4 GO and KEGG functional enrichment analyses based on the DEGs. (A) Bubble plot of biological processes in the GO enrichment analysis. (B) The directed acyclic graph of biological process in the GO enrichment analysis. (C) Bubble plot of pathways in the KEGG enrichment analysis.

Figure 5 (A) Laser confocal scanning microscopy images of FYGL in 3T3-L1 cells at 200× magnification. 3T3-L1 cells were incubated with FITC–FYGL (200 µg/mL) for 4 h; blue (DAPI labelled), red (rhodamine labelled) and green (FITC labelled) represent the nucleus, cytoskeleton and FYGL, respectively. The scale bar represents 100 µm. (B) Flow cytometric analysis of fluorescence. (C) Geometric means calculated by FlowJo software. The data are presented as the mean \pm S.D. values (n = 3). *** $P < 0.001 \ vs$. control group. (D) Effect of FYGL on cell viability. 3T3-L1 cells were incubated with various concentrations of FYGL (0, 50, 100, 200, 400 and 800 µg·mL⁻¹) for 24 h, and cell viability was determined by a CCK-8 assay. The mean \pm S.D. values are presented (n = 6)

(A)

(B)

(C)

Figure 6 Effect of *FYGL* on the inhibition of lipid accumulation in mature adipocytes. Differentiated 3T3-L1 cells were incubated with *FYGL* at concentrations ranging from 0–400 µg/mL. (A) Intracellular TG in mature adipocytes. (B) Intracellular lipid droplets stained by oil red O and visualized by polarized phase contrast microscopy (500×). (C) Intracellular lipid accumulation was quantitatively measured using a microplate reader at an absorbance of 490 nm. Mean \pm S.D. values are presented (n = 6). ###P < 0.001 vs. blank control group, **P < 0.01, *P < 0.05 vs. model group.

Figure 7 The relative mRNA expression levels of (A) C/EBPα, (B) FABP-4, (C) ATGL, and (D) LPL in differentiated 3T3-L1 cells, with reference to the model group. Data are presented as the mean \pm S.D. values (n = 6). ****P < 0.001, ***P < 0.01, **P < 0.05 vs. blank control group. ****P < 0.001, **P < 0.01, **P < 0.05 vs. model group

Figure 8 Western blot analysis of proteins involved in cellular differentiation in mature 3T3-L1 cells. (A) Images of the PPAR γ , C/EBP α , and FABP-4 protein bands relative to the β -actin protein band. (B), (C) and (D) Relative expression of PPAR γ , C/EBP α , and FABP-4, respectively, with reference to β -actin, and normalized to the model group. Data are presented as the mean \pm S.D. values (n = 3). *#P < 0.01, *P < 0.05 vs. blank control group, ****P < 0.001, **P < 0.01, *P < 0.05 vs. model group.

Figure 9 Western blot analysis of proteins involved in lipolysis and the AMPK α signalling pathway in mature 3T3-L1 cells. (A) Image of FAS protein bands, (B) Quantification of FAS expression. (C) Images of ATGL, HSL, LPL, p-AMPK α , and AMPK α protein bands. (D), (E), (F) and (G) Quantification of ATGL, HSL, LPL, and p-AMPK α /AMPK α protein levels. The protein levels in the model group are normalized to a value of 1.0. Data are presented as the mean \pm S.D. values (n = 3). *##P < 0.01, *##P < 0.001 vs. blank control group, **P < 0.01, *P < 0.05 vs. model group.

681	
001	Figure 10 Profile of the mechanism of $FYGL$ in ameliorating diabetes-associated obesity

20230405201350841085309659541504

ORIGINALITY REPORT

40%

SIMILARITY INDEX

PRIMARY SOURCES

- $\frac{\text{www.mdpi.com}}{\text{Internet}} 300 \, \text{words} 5\%$
- academic.oup.com $_{\text{Internet}}$ 250 words -4%
- $\frac{\text{www.biorxiv.org}}{\text{Internet}}$ 133 words 2%
- Mengqing Wu, Dan Liu, Rong Zeng, Tao Xian, Yi Lu, Guohua Zeng, Zhangzetian Sun, Bowei Huang, Qiren Huang. "Epigallocatechin-3-gallate inhibits adipogenesis through down-regulation of PPARy and FAS expression mediated by PI3K-AKT signaling in 3T3-L1 cells", European Journal of Pharmacology, 2017
- scholarworks.umass.edu 87 words 1 %
- Shilin Yuan, Yanna Pan, Zeng Zhang, Yanming He, Yilong Teng, Haohui Liang, Xiao Wu, Hongjie Yang, Ping Zhou. "Amelioration of the lipogenesis, oxidative stress and apoptosis of hepatocytes by a novel proteoglycan from <i>Ganoderma lucidum</i>", Biological and Pharmaceutical Bulletin, 2020

7	www.researchgate.net	69 words — 1 %
8	interstellarsuperherbs.com Internet	67 words — 1%
9	Dong Xu, Tao Qiao, Yue Wang, Qiang-Song Wang, Yuan-Lu Cui. "Alginate nanogels-based thermosensitive hydrogel to improve antidepressant effects of albiflorin via intranasal delivery", Drug Deliv	
10	journals.plos.org	48 words — 1 %
11	Yanna Pan, Shilin Yuan, Yilong Teng, Zeng Zhang et al. "Antioxidation of a proteoglycan from Ganoderma lucidum protects pancreatic β-cells against oxidative induced apoptosis in vitro and in vivo", International Biological Macromolecules, 2022	stress-
12	pubs.rsc.org Internet	37 words — 1%
13	www.hindawi.com Internet	37 words — 1%
14	www.researchsquare.com Internet	34 words — 1%
15	lipidworld.biomedcentral.com Internet	30 words — 1 %
16	www.frontiersin.org	30 words — 1 %

- Yang Jiang, Shijie Ding, Feng Li, Chen Zhang, Dongxiao Sun-Waterhouse, Yilun Chen, Dapeng Li. "Effects of (+)-catechin on the differentiation and lipid metabolism of 3T3-L1 adipocytes", Journal of Functional Foods, 2019

 Crossref
- Shilin Yuan, Yanna Pan, Zeng Zhang, Yanming He, Yilong Teng, Haohui Liang, Xiao Wu, Hongjie Yang, Ping Zhou. "Amelioration of the Lipogenesis, Oxidative Stress and Apoptosis of Hepatocytes by a Novel Proteoglycan from <i>Ganoderma lucidum</i>", Biological and Pharmaceutical Bulletin, 2020
- www.spandidos-publications.com $_{\text{Internet}}$ 23 words -<1%
- Yanna Pan, Ying Zhang, Jiaqi Li, Zeng Zhang, Yanming He, Qingjie Zhao, Hongjie Yang, Ping Zhou. "A proteoglycan isolated from Ganoderma lucidum attenuates diabetic kidney disease by inhibiting oxidative stress-induced renal fibrosis both in vitro and in vivo", Journal of Ethnopharmacology, 2023

 Crossref
- Ying Zhang, Yanna Pan, Jiaqi Li, Zeng Zhang, Yanming He, Hongjie Yang, Ping Zhou. "Inhibition on α -Glucosidase Activity and Non-Enzymatic Glycation by an Anti-Oxidative Proteoglycan from Ganoderma lucidum", Molecules, 2022 Crossref
- Zhou Yang, Fan Wu, Yanming He, Qiang Zhang, Yuan Zhang, Guangrong Zhou, Hongjie Yang, Ping 20 words <1% Zhou. " A novel PTP1B inhibitor extracted from ameliorates

insulin resistance by regulating IRS1-GLUT4 cascades in the insulin signaling pathway ", Food & Function, 2018

Crossref

	mdpi-res.com Internet	$_{20\mathrm{words}}$ $ <$ 1%
--	-----------------------	----------------------------------

- Junpei Yamamoto, Takumi Yamane, Yuichi Oishi, Kazuo Kobayashi-Hattori. "Perfluorooctanoic acid binds to peroxisome proliferator-activated receptor γ and promotes adipocyte differentiation in 3T3-L1 adipocytes", Bioscience, Biotechnology, and Biochemistry, 2014
- Metabolic Syndrome, 2016.

 19 words < 1%atvb.ahajournals.org
 Internet

 19 words < 1%19 words < 1%
- res.mdpi.com
 19 words < 1 %
- Yilong Teng, Haohui Liang, Zeng Zhang, Yanming He, Yanna Pan, Shilin Yuan, Xiao Wu, Qingjie Zhao, Hongjie Yang, Ping Zhou. "Biodistribution and immunomodulatory activities of a proteoglycan isolated from Ganoderma lucidum", Journal of Functional Foods, 2020 Crossref

$$_{18 \text{ words}}$$
 $< 1\%$

31	Bao, Qinwen, Xiaozhu Shen, Li Qian, Chen Gong, Maoxiao Nie, and Yan Dong. "Anti-diabetic activities of catalpol in db/db mice", Korean Journ Physiology and Pharmacology, 2016. Crossref	17 words — < 1% nal of
32	foodandnutritionresearch.net	17 words — < 1 %
33	worldwidescience.org	17 words — < 1 %
34	www.cellandbioscience.com	17 words — < 1 %

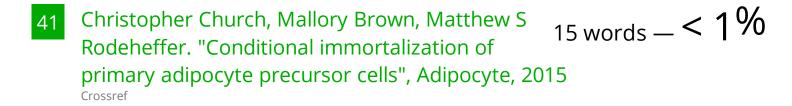
35	www.wjgnet.com Internet	17 words — < 1 %

"The Lingzhi Mushroom Genome", Springer Science and Business Media LLC, 2021
$$^{\text{Crossref}}$$
 16 words — $< 1\%$

Ji Young Je, Jae Eun Park, Youngwan Seo, Ji Sook Han. "HM-chromanone inhibits adipogenesis by regulating adipogenic transcription factors and AMPK in 3T3-L1 adipocytes", European Journal of Pharmacology, 2021 Crossref

aac.asm.org
$$_{\text{Internet}}$$
 16 words $-<1\%$

clinical proteomics journal. biomed central. com
$$_{\text{Internet}}$$
 16 words $-<1\%$



15 words — < 1% Jinye Huang, Jun Li, Hui Chen, Chensi Shen, Yuezhong Wen. "Ecological Toxicity Alleviation of Imazethapyr to Non-target Plant Wheat: Active Regulation Between Auxin and DIMBOA", Research Square Platform LLC,

Crossref Posted Content

 $_{15 \text{ words}}$ - < 1%Kang Song, Yifan Zhang, Qin Ga, Zhenzhong Bai, 43 Ri-Li Ge. "High-altitude chronic hypoxia ameliorates obesity-induced non-alcoholic fatty liver disease in mice by regulating mitochondrial and AMPK signaling", Life Sciences, 2020

Crossref

44koreascience.kr
Internet
$$15 \text{ words} - < 1\%$$
45kclpure.kcl.ac.uk
Internet $14 \text{ words} - < 1\%$ 46hwmaint.fasebj.org
Internet $13 \text{ words} - < 1\%$ 47link.springer.com
Internet $13 \text{ words} - < 1\%$ 48d197for5662m48.cloudfront.net
Internet $12 \text{ words} - < 1\%$

www.intechopen.com Internet

48

 $_{12 \text{ words}} - < 1\%$

- Yu-Shan Hsiao, Gerwald Jogl, Victoria Esser, Liang $_{11}$ words <1% Tong. "Crystal structure of rat carnitine palmitoyltransferase II (CPT-II)", Biochemical and Biophysical Research Communications, 2006
- Hao Huang, Tarun Belwal, Li Li, Yanqun Xu, Ligen Zou, Xingyu Lin, Zisheng Luo. "Amphiphilic and Biocompatible DNA Origami Based Emulsion Formation and Nanopore Release for Anti Melanogenesis Therapy", Small, 2021 Crossref
- Lau, P., Z. K. Tuong, S.-C. Wang, R. L. Fitzsimmons, J. Goode, G. P. Thomas, G. J. Cowin, M. A. Pearen, K. Mardon, J. L. Stow, and G. E. O. Muscat. "Ror deficiency and decreased adiposity are associated with induction of thermogenic gene expression in subcutaneous white and brown adipose tissue.", AJP Endocrinology and Metabolism, 2014.

Menghua Zhang, Xiaoxue Liu, Zhiyao Chen, Shenhao Jiang, Lin Wang, Min Tao, Liyan Miao. "Method development and validation for simultaneous determination of six tyrosine kinase inhibitors and two active metabolites in human plasma/serum using UPLC-MS/MS for therapeutic drug monitoring", Journal of Pharmaceutical and Biomedical Analysis, 2021

 $_{10\,\mathrm{words}}$ $_{-}$ < 1%

bmccomplementmedtherapies.biomedcentral.com

Crossref

shareok.org

10 words -<1%

57 www.sciencegate.app

- 10 words -<1%
- Ae Park, S.. "Genistein and daidzein modulate hepatic glucose and lipid regulating enzyme activities in C57BL/KsJ-db/db mice", Life Sciences, 20060815 $^{\text{Crossref}}$
- Eva García-Escobar. "Effect of insulin analogues on $_{9~words}$ <1% 3t3-l1 adipogenesis and lipolysis : INSULIN ANALOGUES ON 3T3-L1 ADIPOGENESIS AND LIPOLYSIS", European Journal of Clinical Investigation, 09/2011
- Geng Li, Linghui Zhang. "miR-335-5p aggravates type 2 diabetes by inhibiting SLC2A4 expression",

 Biochemical and Biophysical Research Communications, 2021

 Crossref
- Jun Shu, Nan Li, Wenshi Wei, Li Zhang. "Detection of molecular signatures and pathways shared by Alzheimer's disease and type 2 diabetes", Gene, 2021 Crossref
- Jung Seok HWANG, Su Bi LEE, Mi-Jung CHOI, Jun Tae KIM, Han Geuk SEO. "Anti-adipogenic effect of a turmeric extract-loaded nanoemulsion in 3T3-L1 preadipocytes and high fat diet-fed mice", Food Science and Technology, 2019

 Crossref



- Reddy Sankaran Karunakaran, Oruganti
 Lokanatha, Ganjayi Muni Swamy, Chintha
 Venkataramaiah et al. "Anti-Obesity and Lipid Lowering Activity
 of Bauhiniastatin-1 is Mediated Through PPAR-γ/AMPK
 Expressions in Diet-Induced Obese Rat Model", Frontiers in
 Pharmacology, 2021
 Crossref
- Yue Tong, Sai Xu, Lili Huang, Chen Chen. "Obesity and insulin resistance: pathophysiology and treatment", Drug Discovery Today, 2021

 Crossref
- bmcpsychiatry.biomedcentral.com 9 words < 1%
- 67 hdl.handle.net 9 words < 1 %
- jneuroinflammation.biomedcentral.com 9 words < 1%
- tessera.spandidos-publications.com 9 words < 1%
- www.dovepress.com

 Internet

 9 words < 1 %
- www.nature.com

 Internet

 9 words < 1 %

72	www.scielo.br
	Internet

9 words - < 1%

73 www.tesisenred.net

- 9 words < 1%
- "Cell Biology and Translational Medicine, Volume 2", Springer Science and Business Media LLC, 2018 8 words < 1%
- Rulifson, I. C., J. Z. Majeti, Y. Xiong, A. Hamburger, 8 words < 1 % K.-J. Lee, L. Miao, M. Lu, J. Gardner, Y. Gong, H. Wu, R. Case, W.-C. Yeh, W. G. Richards, H. Baribault, and Y. Li. "Inhibition of Secreted Frizzled-Related Protein 5 Improves Glucose Metabolism", AJP Endocrinology and Metabolism, 2014.
- Yuli Zhang, Ni Chai, Zhenzhen Wei, Zan Li et al. "YYFZBJS inhibits colorectal tumorigenesis by enhancing Tregs-induced immunosuppression through HIF-1 α mediated hypoxia in vivo and in vitro", Phytomedicine, 2022 Crossref
- Zhou Yang, Congheng Chen, Juan Zhao, Weijie Xu, Yanming He, Hongjie Yang, Ping Zhou. "Hypoglycemic mechanism of a novel proteoglycan, extracted from Ganoderma lucidum, in hepatocytes", European Journal of Pharmacology, 2018

 Crossref
- 78 downloads.hindawi.com

 $8 \, \text{words} \, - < 1 \, \%$

79 jcancer.org

 $8 \, \text{words} \, - < 1 \%$

80	Internet	8 words — <	1	%
81	jitc.bmj.com Internet	8 words — <	1	%
82	mdpi.com Internet	8 words — <	1	%
83	nutritionandmetabolism.biomedcentral.com	8 words — <	1	%
84	opendiabetesjournal.com Internet	8 words — <	1	%
85	revistabionatura.com Internet	8 words — <	1	%
86	waseda.repo.nii.ac.jp Internet	8 words — <	1	%
87	www.science.gov Internet	8 words — <	1	%
88	Angiogenesis in Adipose Tissue, 2013. Crossref	7 words — <	1	%
89	Haohui Liang, Yanna Pan, Yilong Teng, Shilin Yuan, Xiao Wu, Hongjie Yang, Ping Zhou. " A proteoglycan extract from protects pancreatic beta against STZ-induced apoptosis ", Bioscience, Biotec Biochemistry, 2020 Crossref	a-cells	1	%

Zhou Yang, Fan Wu, Hongjie Yang, Ping Zhou. The street Through Throug

extracted from Ganoderma lucidum, in HepG2 cells", RSC Adv., 2017

Crossref

Crossref

- "Mechanisms involved in the loss of brown adipose tissue in the AGPAT2 deficient mouse.", Pontificia Universidad Catolica de Chile, 2019

 Crossref Posted Content
- "Principles of Diabetes Mellitus", Springer Science and Business Media LLC, 2017

 Crossref 6 words -<1%
- Albert Boronat-Toscano, Diandra Monfort-Ferré, Margarita Menacho, Aleidis Caro et al. "Anti-TNF Therapies Suppress Adipose Tissue Inflammation in Crohn's Disease", International Journal of Molecular Sciences, 2022 Crossref
- Lijun Chi, Dorothy Lee, Sharon Leung, Guanlan Hu et al. "Peroxisome loss leads to increased mitochondrial biogenesis and reduced autophagy to preserve mitochondrial function", Research Square Platform LLC, 2023

 Crossref Posted Content
- Medina-Gómez, Gema. "Mitochondria and endocrine function of adipose tissue", Best Practice & Research Clinical Endocrinology & Metabolism, 2012. Crossref
- Min, Byulchorong, Heejin Lee, Ji Hye Song, Myung $_{6 \text{ words}} < 1\%$ Joo Han, and Jayong Chung. "Arctiin inhibits adipogenesis in 3T3-L1 cells and decreases adiposity and body weight in mice fed a high-fat diet", Nutrition Research and Practice, 2014.



Walter Wahli. "Fat poetry: a kingdom for PPARy", Cell Research, 06/2007

 $_{6 \text{ words}}$ - < 1 %

Crossref

EXCLUDE QUOTES OFF EXCLUDE SOURCES OFF
EXCLUDE BIBLIOGRAPHY ON EXCLUDE MATCHES OFF